Effect of process-specific defects on the tensile and constant-amplitude fatigue behavior of as-built Ti-6Al-4V alloy produced by laser powder bed fusion process

Saikumar R. Yeratapally[1], Erik L. Frankforter[2], George R. Weber[2], Peter W. Spaeth[2], Christapher G. Lang[2], Edward H. Glaessgen[2]

[1]National Institute of Aerospace, Hampton, VA, 23666
[2]NASA Langley Research Center, Hampton, VA, 23681

Additive Manufacturing Benchmarks 2022

Bethesda, Maryland, USA

August 15-18, 2022

Outline

- Introduction
- Laser powder-bed fusion (L-PBF) builds
  - *Process parameters*
  - *Build layout/Specimen geometry*
- Characterization: X-Ray computed tomography (CT)
- Mechanical testing
  - *Uniaxial tensile tests*
  - *Fatigue tests*
  - *Analysis of fracture surfaces*
- Crystal plasticity (CP) simulations
  - *Defect-embedded micromechanical simulations*
  - *Influence of sub-surface microstructure*
  - *Validation of CP simulations*

Introduction

- Additive manufacturing (AM) processes like laser powder-bed fusion (L-PBF) produce process-specific defects that lead to sub-optimal performance of safety-critical and load-bearing components.

- Types of defects produced by L-PBF include (but not limited to):
  - Porosity *(focus of the present work)*
  - Surface roughness
  - Balling
  - Micro cracking
  - Significant residual stresses

- Understanding process-structure-property relations in AM materials is essential for qualification and certification purposes

- Effect of process-induced porosity on the mechanical (tensile and fatigue) behavior of as-built Ti-6Al-4V alloy is investigated using testing, characterization, fractography and simulations

- Complementary information from defect-embedded microstructure models is leveraged to understand pore-grain interaction

Outline

- Introduction
- Laser powder-bed fusion (L-PBF) builds
  - *Process parameters*
  - *Build layout/Specimen geometry*
- Characterization: X-Ray computed tomography (CT)
- Mechanical testing
  - *Uniaxial tensile tests*
  - *Fatigue tests*
  - *Analysis of fracture surfaces*
- Crystal plasticity (CP) simulations
  - *Defect-embedded micromechanical simulations*
  - *Influence of sub-surface microstructure*
  - *Validation of CP simulations*

Process Parameters, Build Layout and Specimen Geometry

Process settings for each build

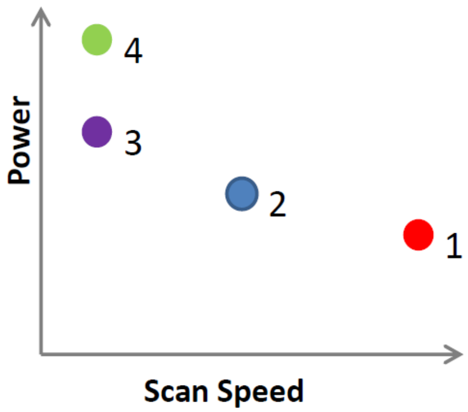

Build ID	Power (W)	Scan Speed (mm/s)	Energy Density (J/mm^3)
1	100	1000	33.33
2	150	750	66.67
3	195	500	130.0
4	270	500	180.0

Build plate containing all four specimens

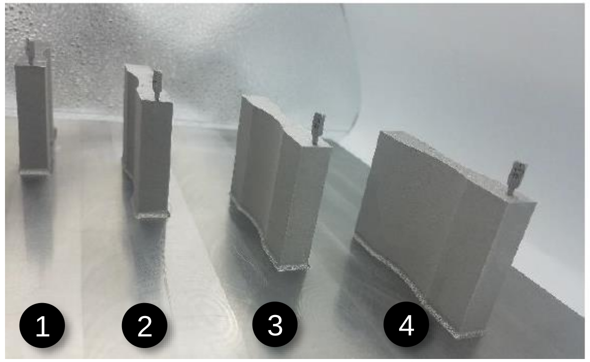

Specimens (4 build IDs) manufactured using:

- Process: L-PBF
- Machine: DMP Flex 350 (3DSystems*)
- Powder: Ti-6Al-4V
- Base plate material: Ti-6Al-4V

Specimen labeling method

***Specimen label**: Build ID-Section ID*

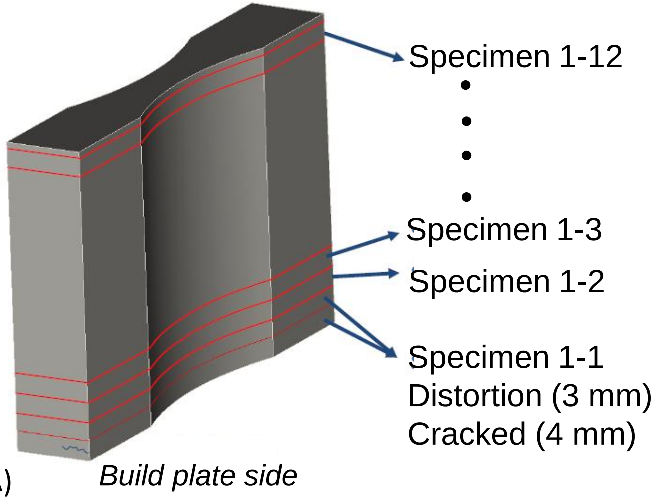

Cross section of specimen

Tensile direction: Y
Build direction: Z

*This is not an endorsement by the National Aeronautics and Space Administration (NASA)

Outline

- Introduction
- Laser powder-bed fusion (L-PBF) builds
  - *Process parameters*
  - *Build layout/Specimen geometry*
- **Characterization: X-Ray computed tomography (CT)**
- Mechanical testing
  - *Uniaxial tensile tests*
  - *Fatigue tests*
  - *Analysis of fracture surfaces*
- Crystal plasticity (CP) simulations
  - *Defect-embedded micromechanical simulations*
  - *Influence of sub-surface microstructure*
  - *Validation of CP simulations*

Characterization: X-Ray CT

X-Ray CT data collected across build conditions for porosity characterization:

- Resolution: 5 μm
- Grayscale image stack: approximately 2000 images, totaling 15 GB per specimen
- Region of interest: 8.5 mm section near midplane
- Specimen section ID: 1-5, 2-5, 3-3, 4-9

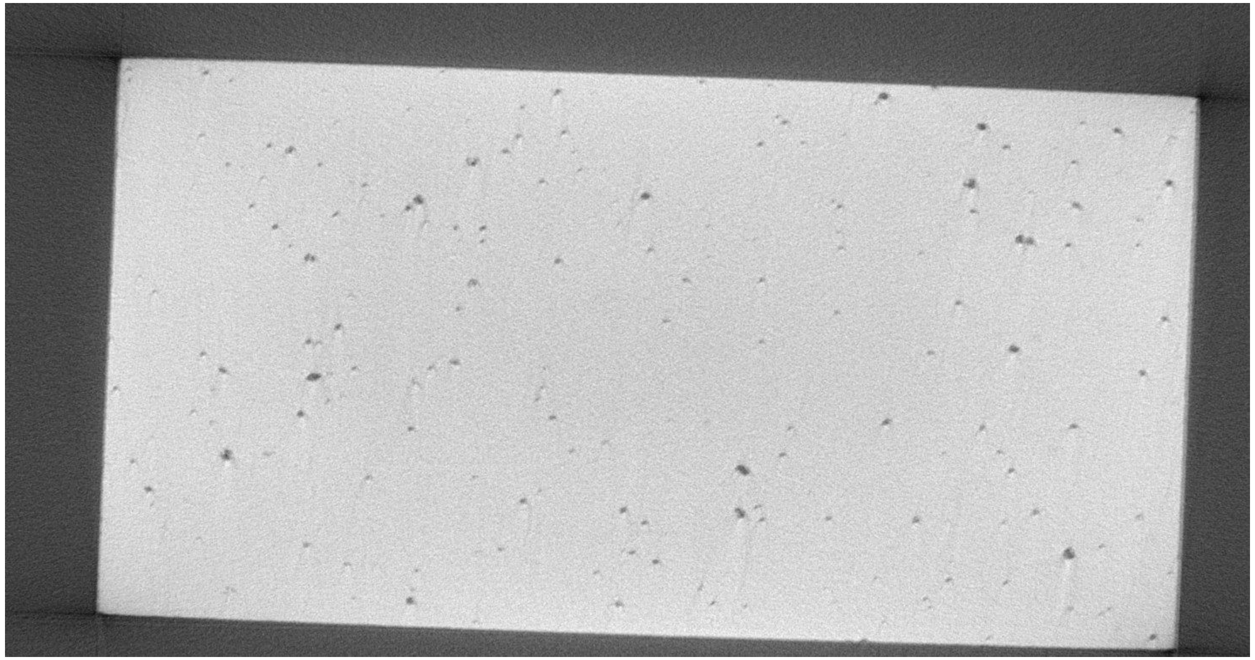

One Z slice of image stack for Specimen 2-5

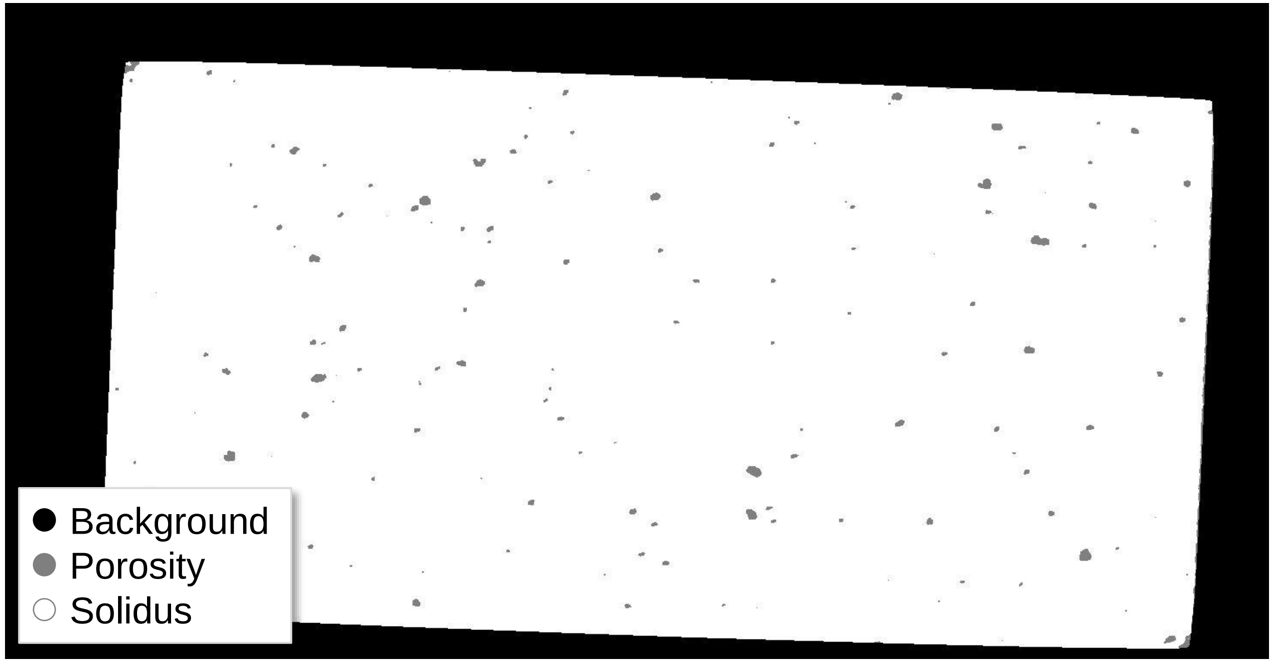

Corresponding segmented image

Random Walker Segmentation

Weighted Graph:

- Vertices: image pixels with intensity g_i
- Edges between neighboring pixels with weights $w_{ij} = \exp\left(-\beta\left(g_i - g_j\right)^2\right)$; β represents a free parameter
- For the unlabeled pixels: assign label k if random walker most likely to first arrive at pixel with label k
- Made computationally feasible by solving a sparse linear system defined by the graph Laplacian

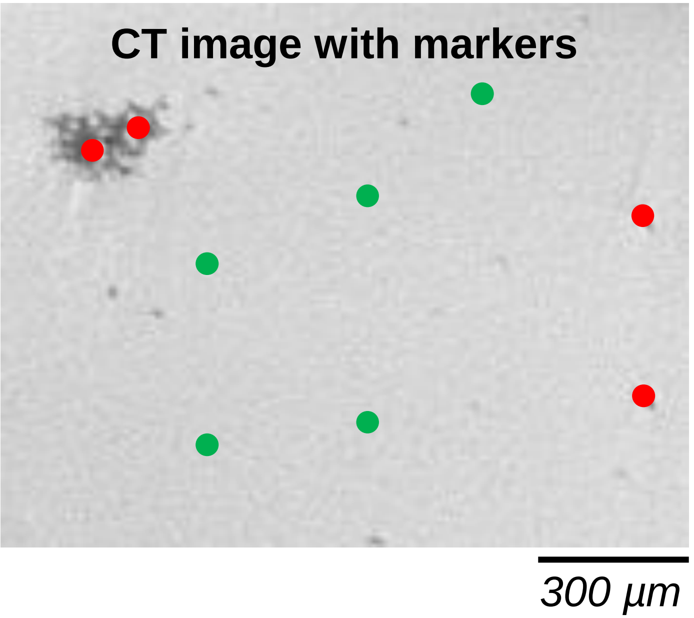

Porosity: ● Solidus: ●

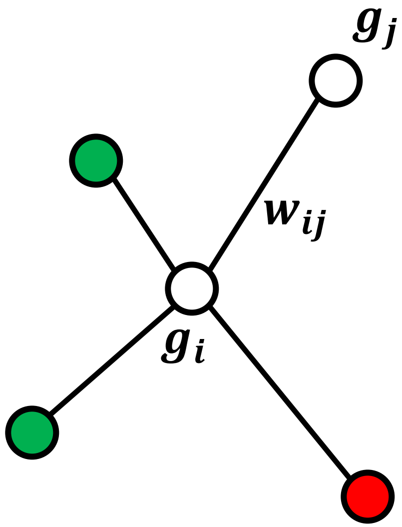

Graph showing connections between labeled and unlabeled pixels

- Leo Grady: Random Walks for Image Segmentation, IEEE Trans Pattern Anal Machine Intel, Vol. 28, No. 11, 2006.
- S. van der Walt, et. al. scikit-image: Image processing in Python.

Characterization: X-Ray CT

Sample results:

- Sample 1-5 has lowest percent porosity and least variability in pore diameter
- Although specimen 3-3 has the highest percent porosity, sample 4-9 has the greatest number of large size pores, and largest pore diameter variability.
- Specimen 1-5 has large pore close to a free surface.
- Correlation with fatigue life data and sensitivity to segmentation parameters are in progress.

Build ID	Power (W)	Scan Speed (mm/s)	Energy Density (J/mm^3)
1	100	1000	33.33
2	150	750	66.67
3	195	500	130.0
4	270	500	180.0

Box and whisker plot of pore size distribution across various builds

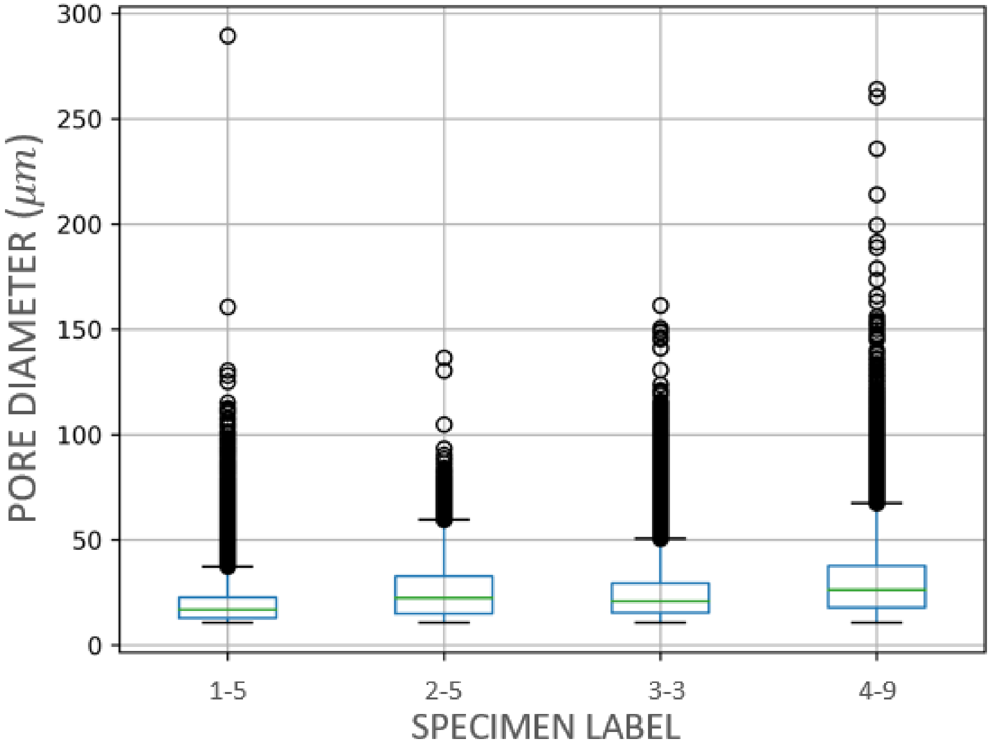

Histogram plot of distribution of pore diameter across various builds

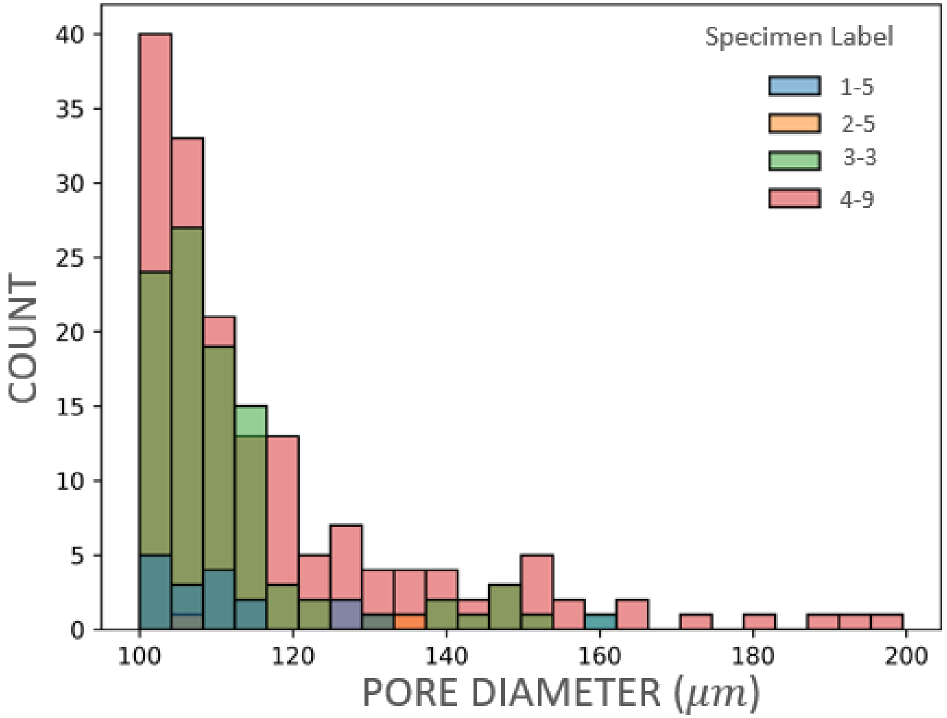

Porosity in a Vicinity of the Free Surface

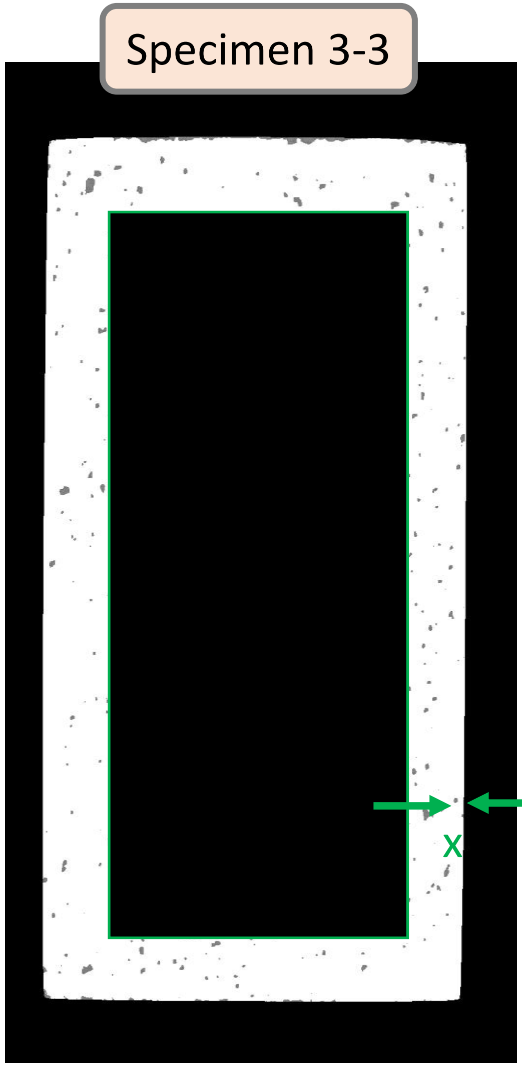

CT image with masked inner section

Build ID	Power (W)	Scan Speed (mm/s)	Energy Density (J/mm³)
1	100	1000	33.33
2	150	750	66.67
3	195	500	130.0
4	270	500	180.0

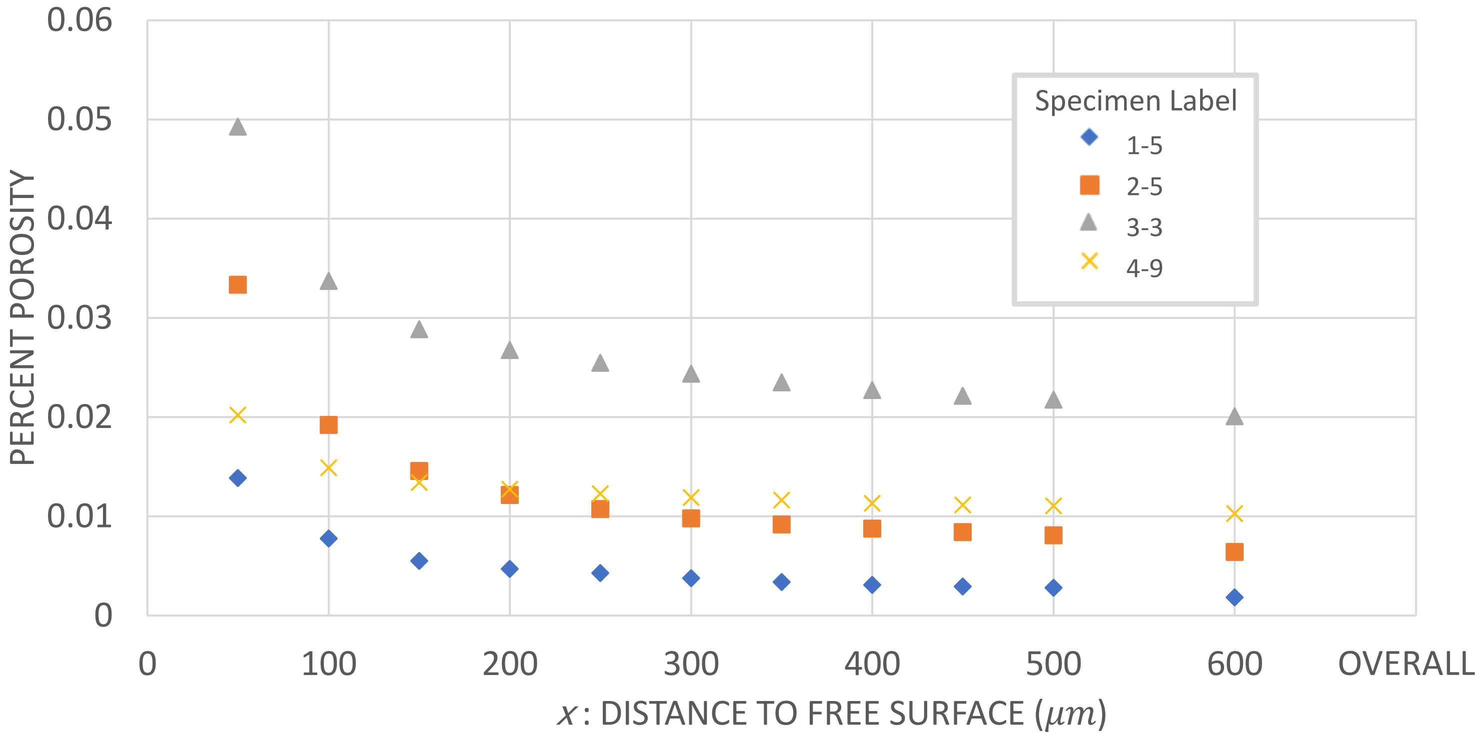

The percentage of porosity decreases away from the free surface

Outline

- Introduction
- Laser powder-bed fusion (L-PBF) builds
  - *Process parameters*
  - *Build layout/Specimen geometry*
- Characterization: *X-Ray computed tomography (CT)*
- **Mechanical testing**
  - *Uniaxial tensile tests*
  - *Fatigue tests*
  - *Analysis of fracture surfaces*
- Crystal plasticity (CP) simulations
  - *Defect-embedded micromechanical simulations*
  - *Influence of sub-surface microstructure*
  - *Validation of CP simulations*

Tensile Behavior

Build ID	Power (W)	Scan Speed (mm/s)	Energy Density (J/mm^3)
1	100	1000	33.33
2	150	750	66.67
3	195	500	130.0
4	270	500	180.0

Tensile behavior

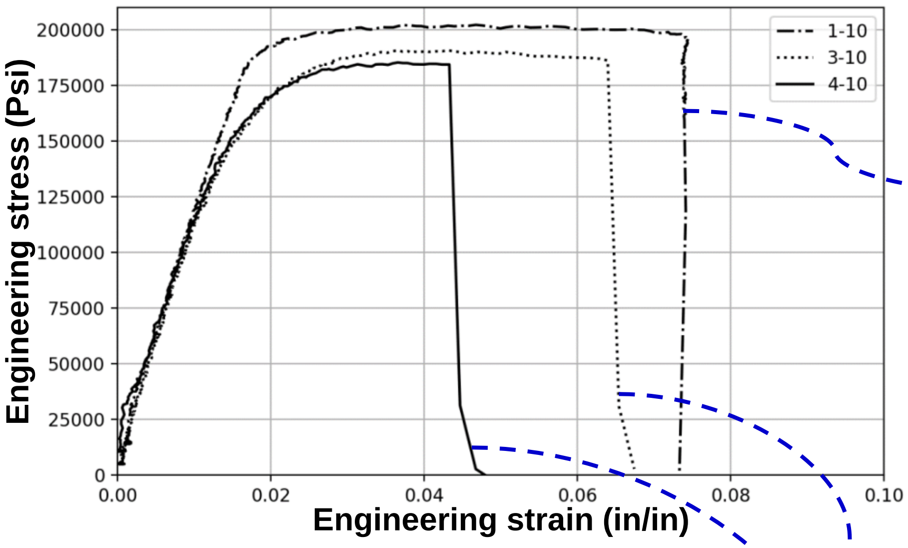

Fracture surfaces of tensile coupons

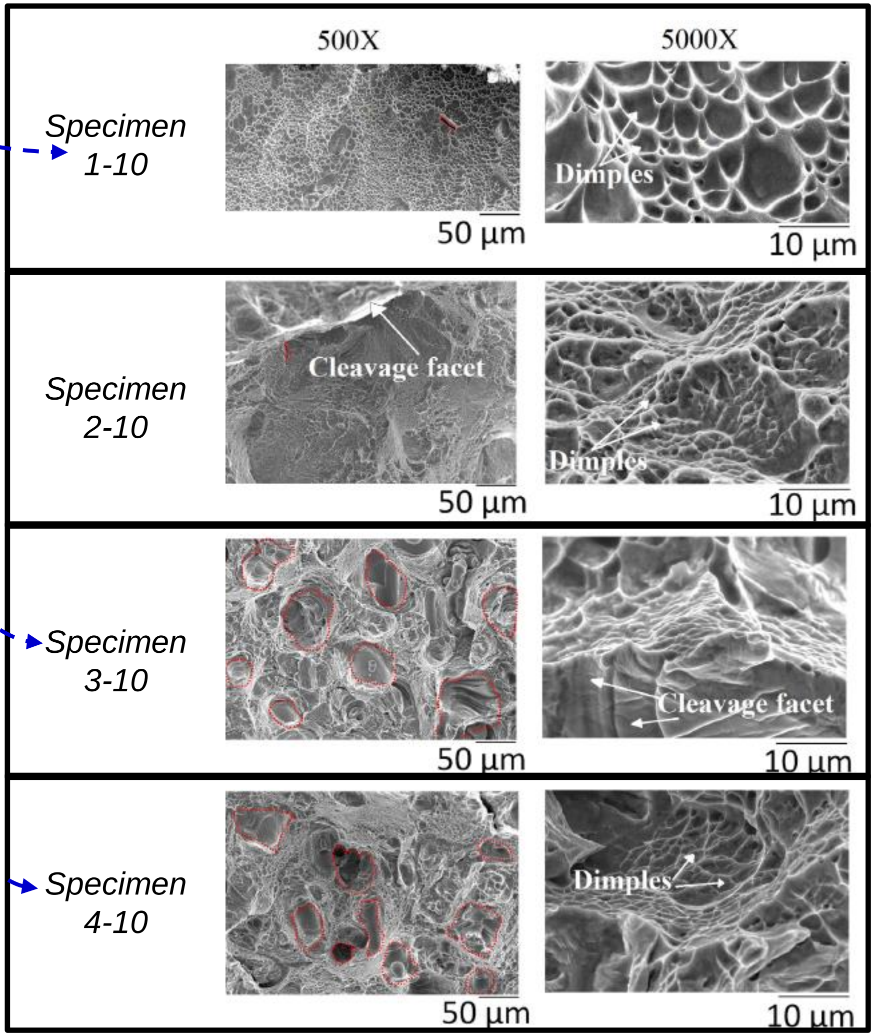

- Strain to failure of coupon 1-10 is 7.64% and that of coupon 4-10 is 4.64%
- Strain-to-failure (ductility) inversely correlates with the amount of porosity
- Fracture surface of coupon 1-10 reveal deeper and wider ductile dimples which result in relatively larger ductility
- Fracture surfaces of coupons 3-10 and 4-10 intersect with large number of process-specific pores

Fatigue Behavior

- 8 coupons, 2 per build, were subjected to fatigue loading at room temperature
- Low cycle fatigue regime was chosen for this study
- Maximum load of 17.2 kN (38.7 lbf) stress ratio of 0.1 and frequency 10 Hz
- Maximum gage stress was approximately 815 MPa
- All specimens failed at the gage

Observation 1: Fatigue lives were significantly lower for coupons from builds with high energy density (Builds 3 and 4), which had a relatively high porosity content

Observation 2: Fracture surfaces of coupons from higher energy densities (Build 3 and 4) intersected with significant number of pores compared to those from lower energy density builds (Build 1 and 2)

Low cycle fatigue behavior for each build

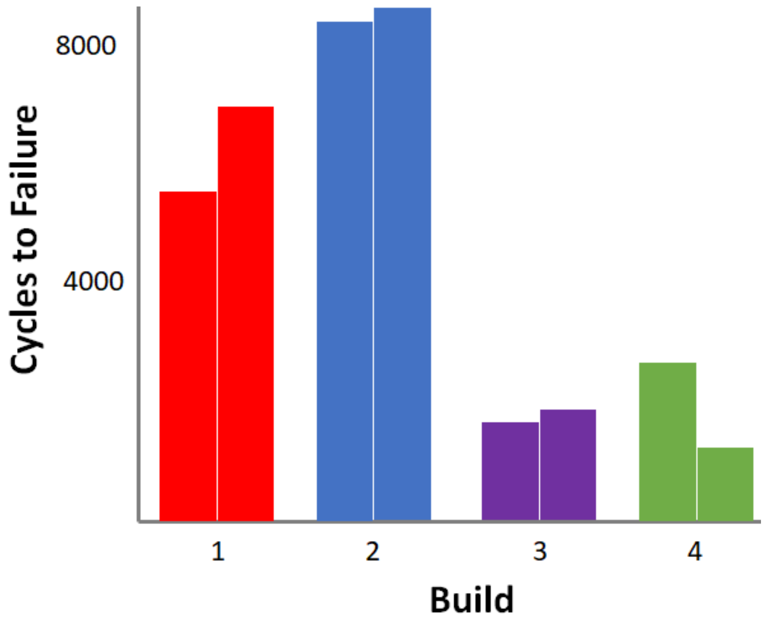

Pore

Specimen 1-12 *Specimen 2-12* *Specimen 3-12* *Specimen 4-12*

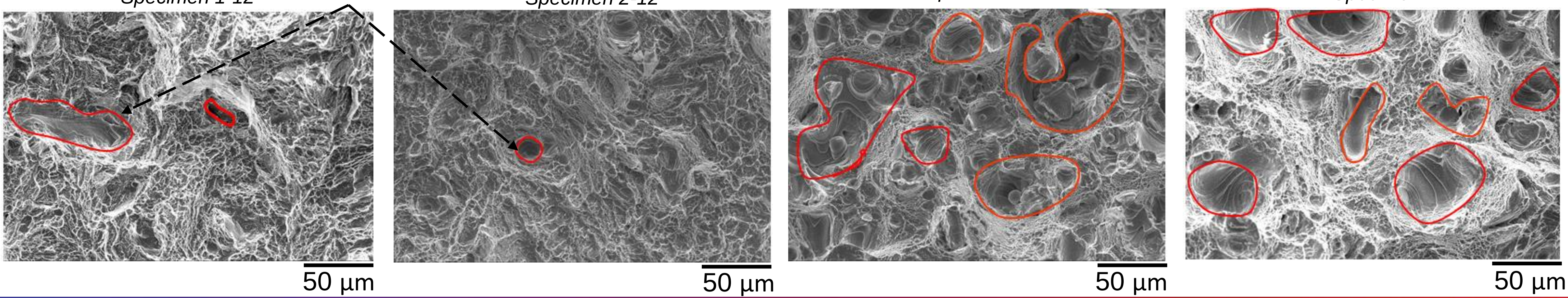

Outline

- Introduction
- Laser powder-bed fusion (L-PBF) builds
  - *Process parameters*
  - *Build layout/Specimen geometry*
- Characterization: *X-Ray computed tomography (CT)*
- Mechanical testing
  - *Uniaxial tensile tests*
  - *Fatigue tests*
  - *Analysis of fracture surfaces*
- **Crystal plasticity (CP) simulations**
  - *Defect-embedded micromechanical simulations*
  - *Influence of sub-surface microstructure*
  - *Validation of CP simulations*

Crystal Plasticity Simulations

- Plasticity simulations are performed to obtain complementary information with regards defect-influenced heterogeneous strain accumulation
- J2 plasticity simulations ignore the influence of the microstructure and hence do not provide insights on the pore-grain interactions
- CP simulation gives quantitative information on the heterogeneous distribution of stress and strain, governed by microstructure and defects
- Fuse the defect and microstructure data to feed the process-specific defect embedded microstructure model into a CP simulation

<u>**Impact**</u>:

- Successful integration of defect and microstructure data to study the effect of defect distribution on strain localization.
- This capability aids in rapid qualification and certification efforts
- Integrates complementary characterization data from X-ray CT and electron backscatter diffraction (EBSD) to gain fundamental understanding on strain localization near defects. This information cannot be obtained by testing alone.

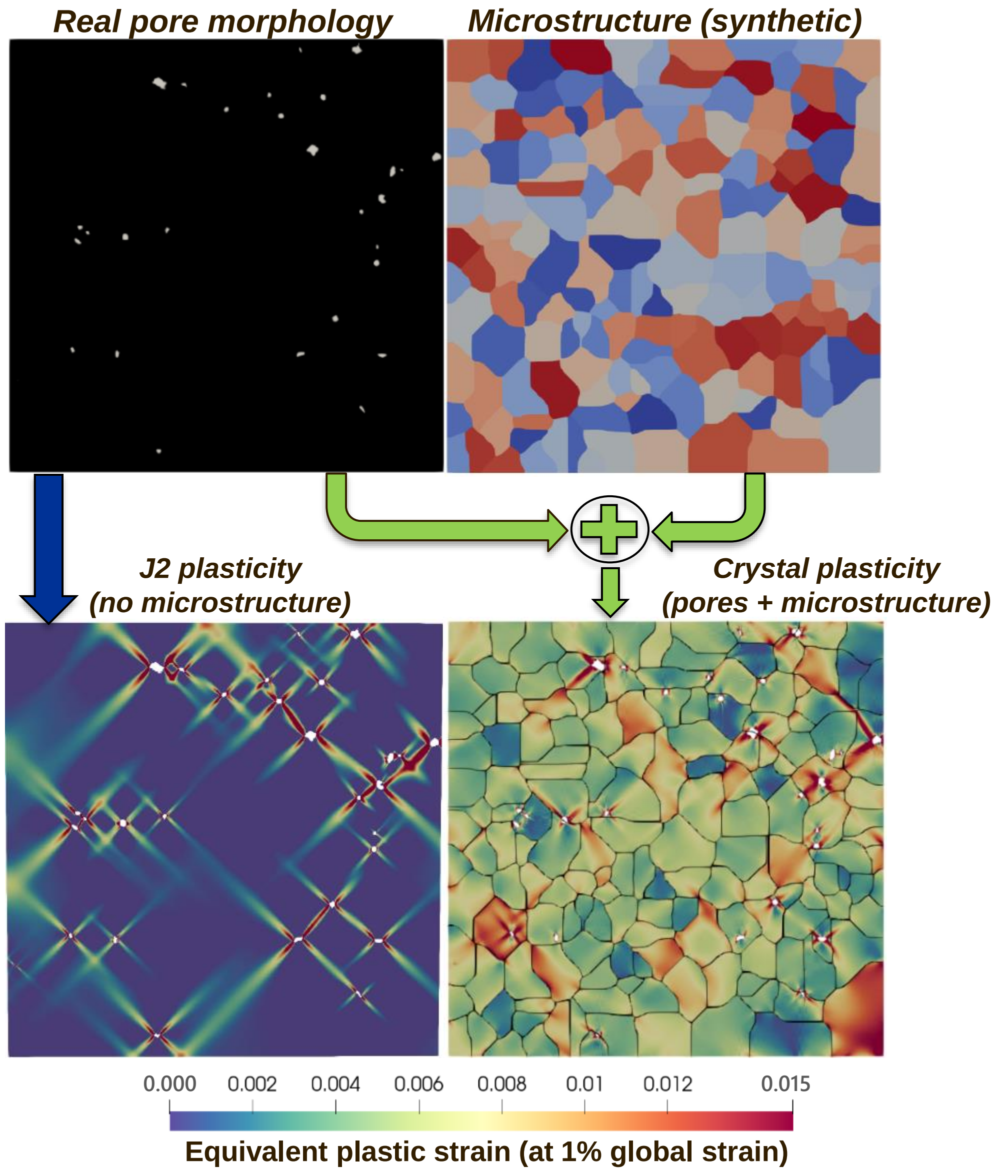

Influence of Pore Neighborhood

Equivalent plastic strain map
(at 1% global strain)

L-PBF process-specific pores in as-built Ti-6Al-4V alloy, obtained from backscatter electron images of metallographic sections

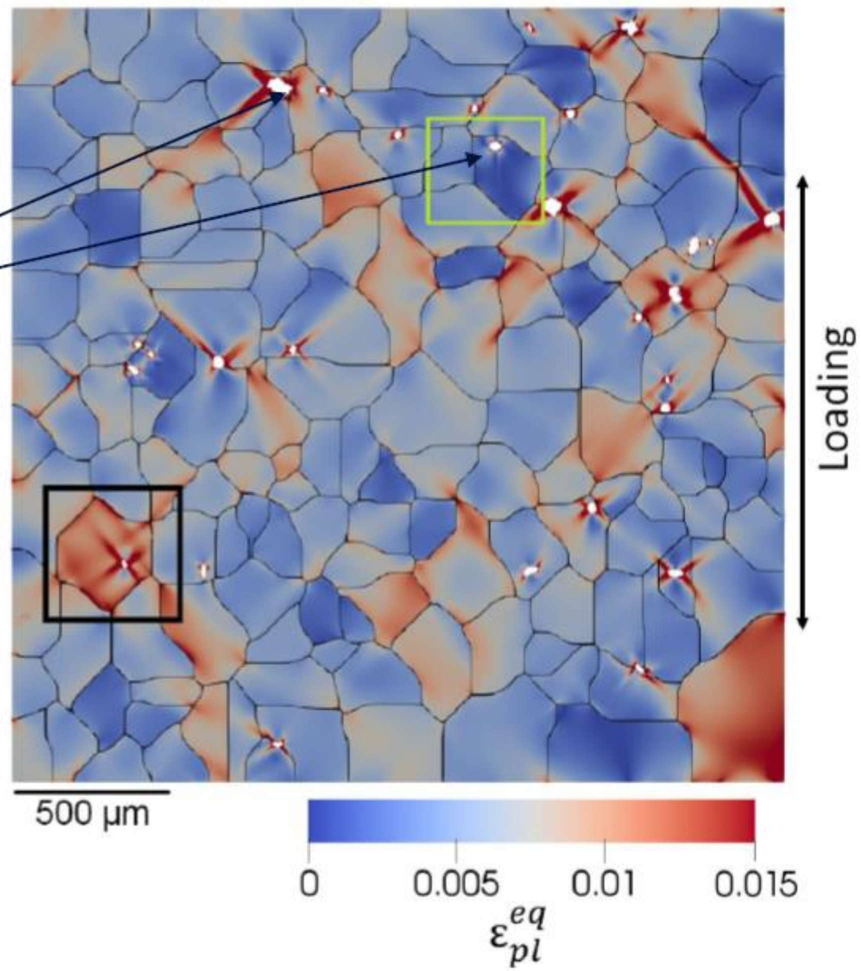

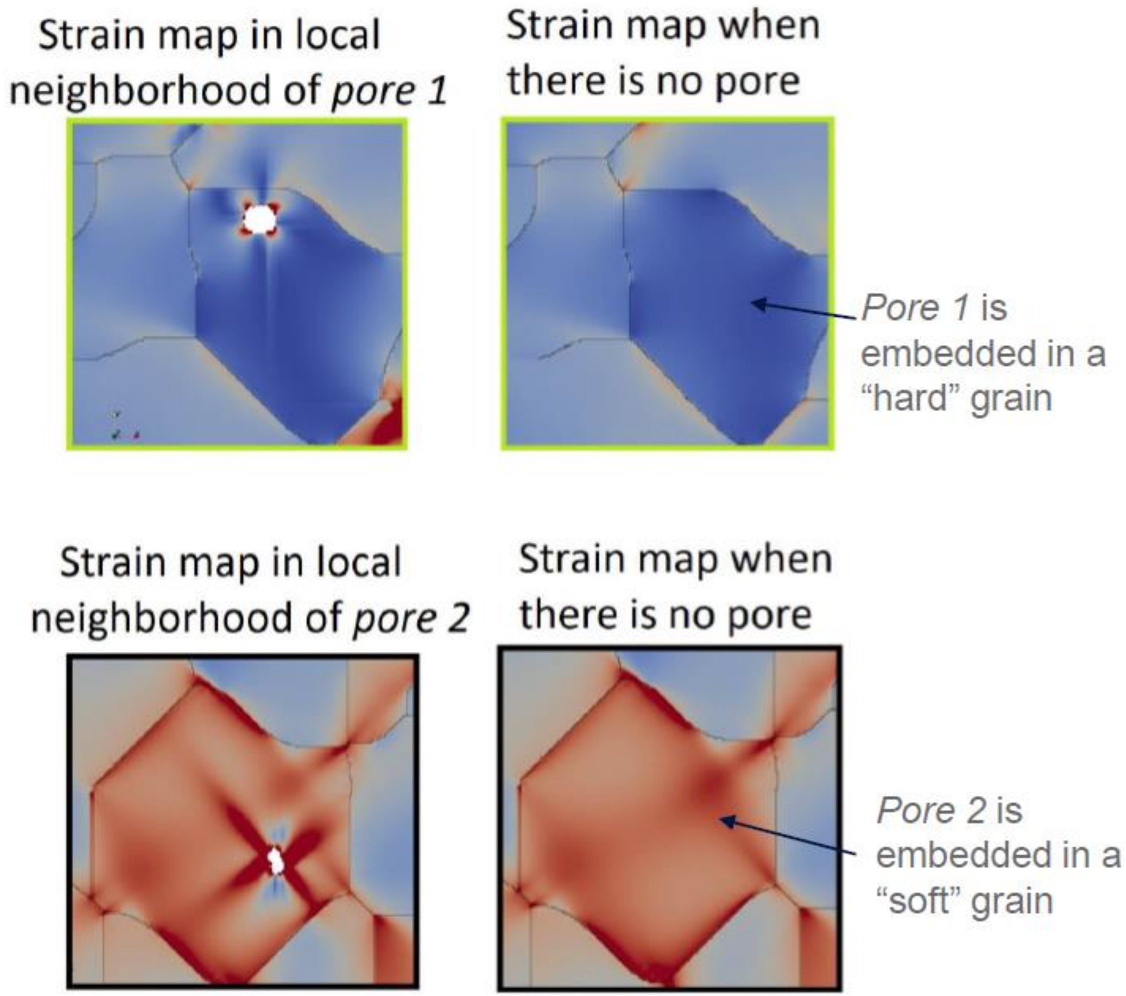

Influence of Pore Neighborhood

Strain map in local neighborhood of *pore 1*

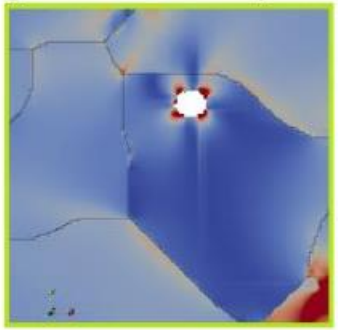

Strain map when there is no pore

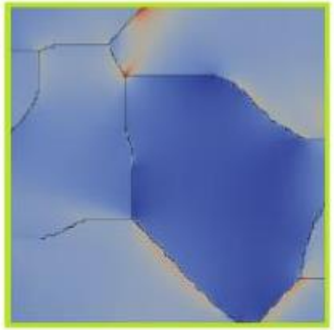

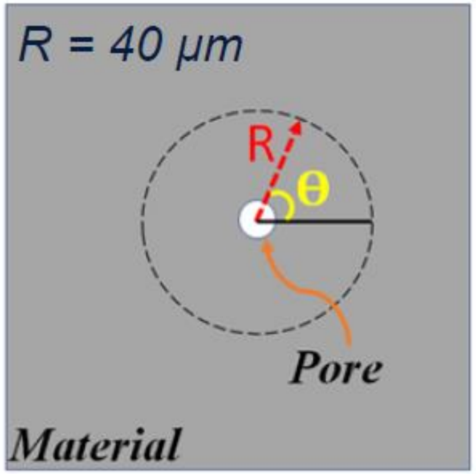

Strain map in local neighborhood of *pore 2*

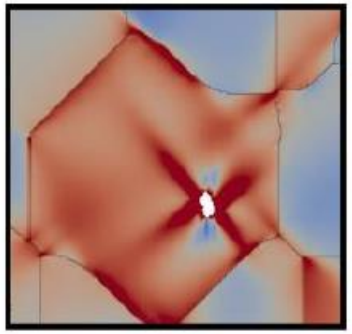

Strain map when there is no pore

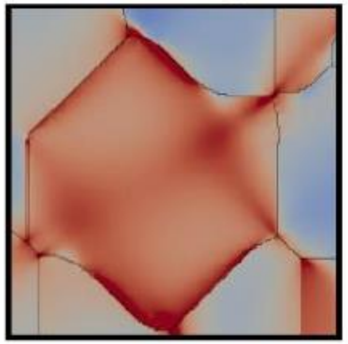

Comparing strain accumulation in vicinity of two pores

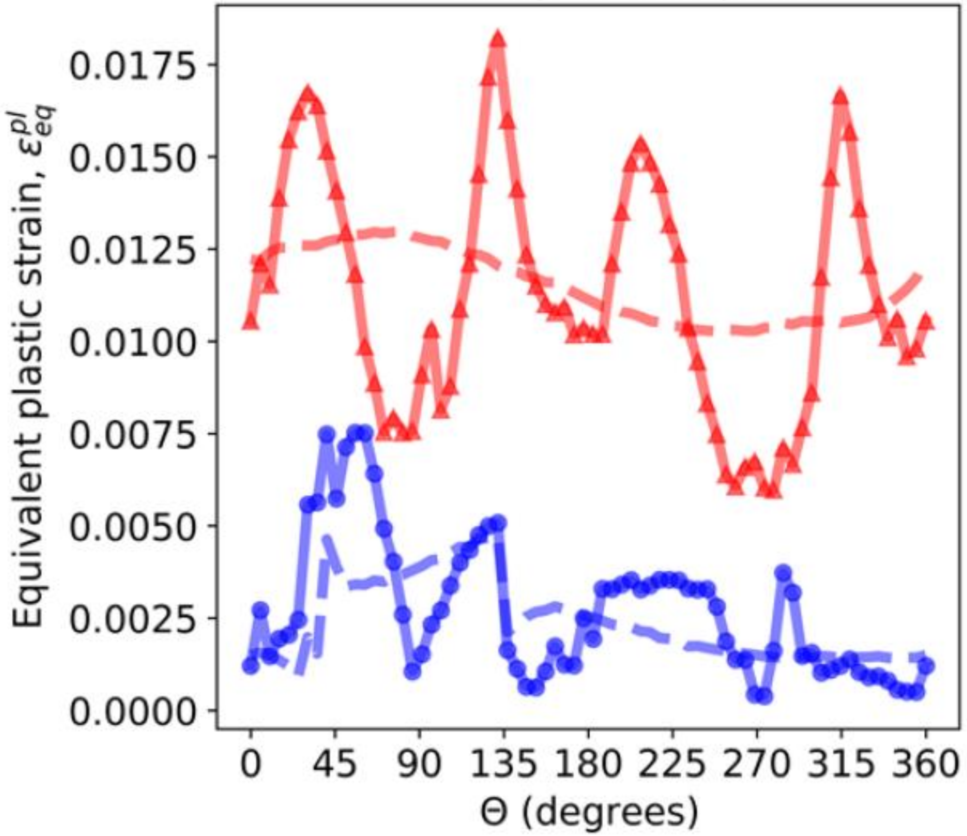

<u>**Observation**</u>: Pore fully embedded in "soft" grain accumulates significant plastic strain in its vicinity compared to a similar sized pore located within a "hard" grain

3-dimensional (3D) Crystal Plasticity Simulations

- Ti-6Al-4V obtained via Electron Powder Bed Fusion [R1]
- Serial sectioning (plasma focused ion beam (PFIB)) coupled with EBSD microscopy were used to collect high resolution crystallographic measurements and reconstruct volumetrically the Ti-6Al-4V microstructure
- Microstructure volume: 256 x 256 x 140 voxels
- Voxel size: 0.1 x 0.1 x 0.1 μm
- CP simulations on serially sectioned microstructure of additively produced Ti-6Al-4V alloy

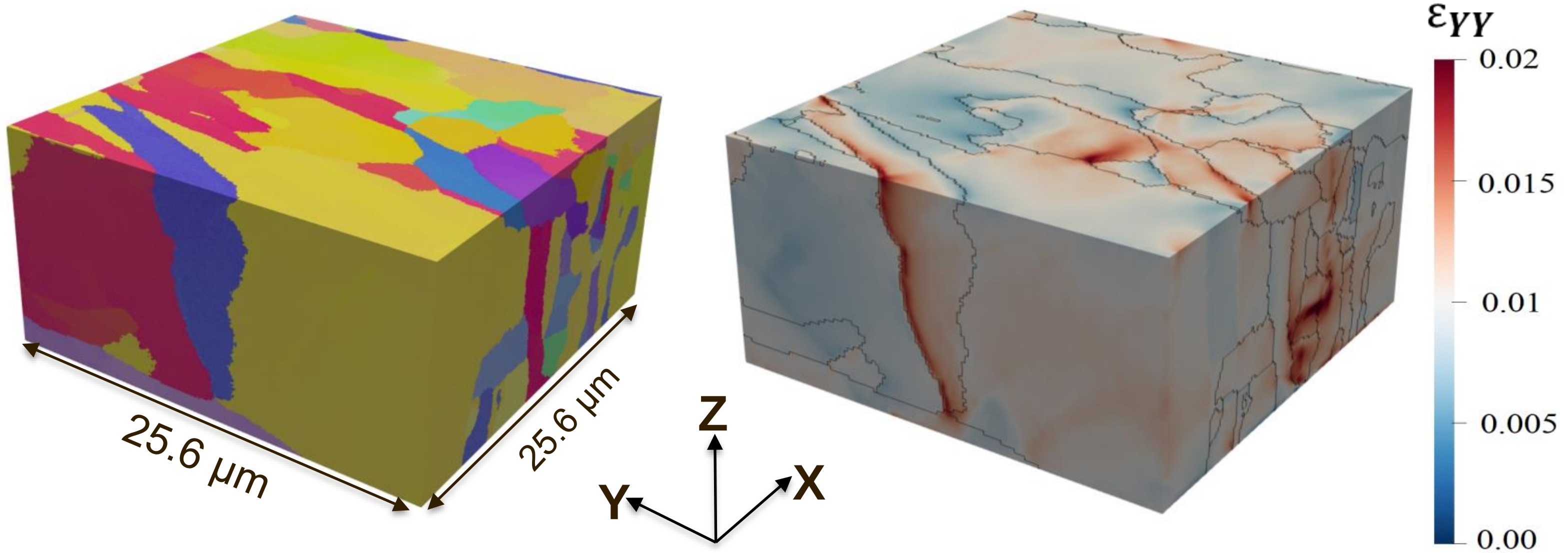

R1: DeMott, Ryan; Primig, Sophie (2021), "3D-EBSD data and analysis of Ti-6Al-4V fabricated using electron powder bed fusion with a random scan strategy (R3)", Mendeley Data, V1, doi: 10.17632/c5x7ckcfsp.1

Influence of Sub-Surface Microstructure

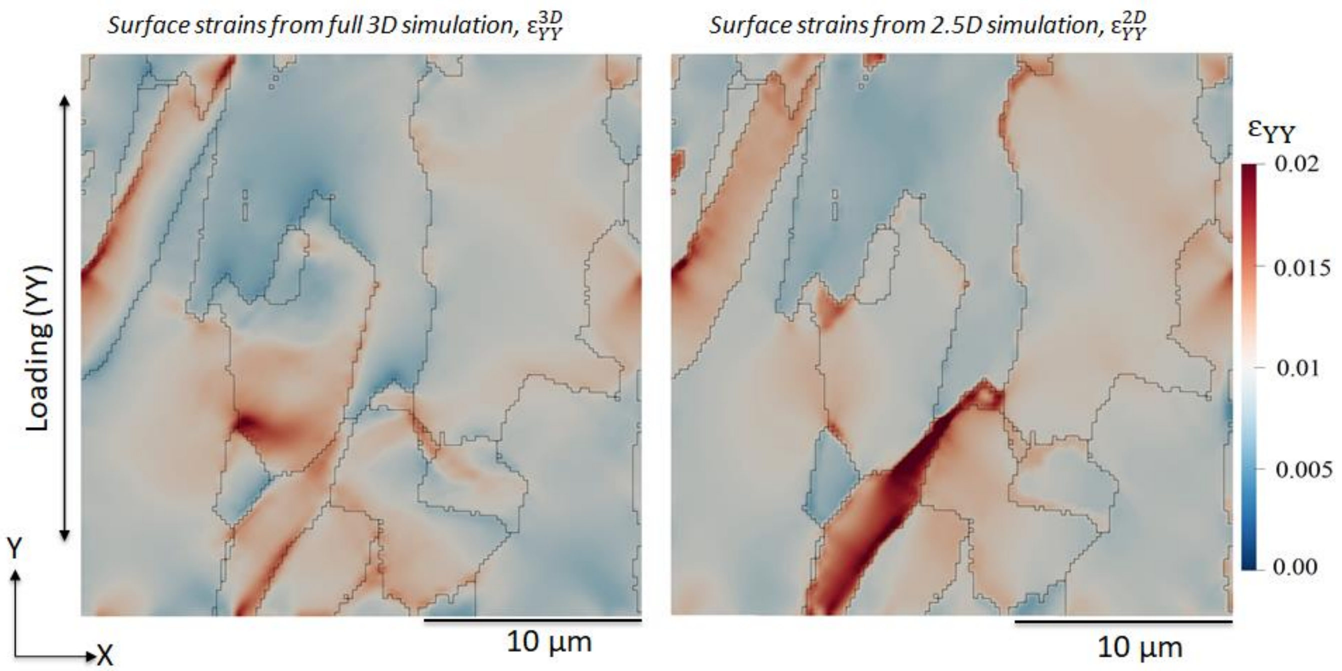

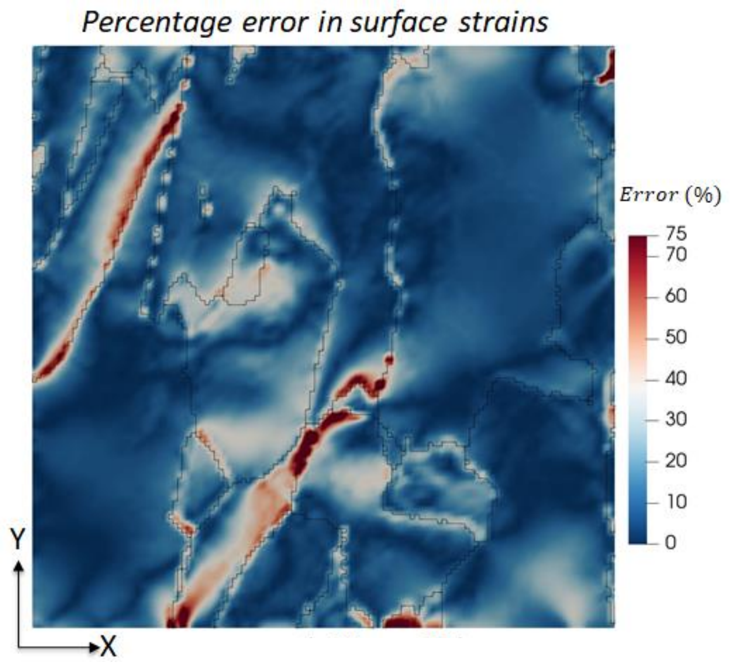

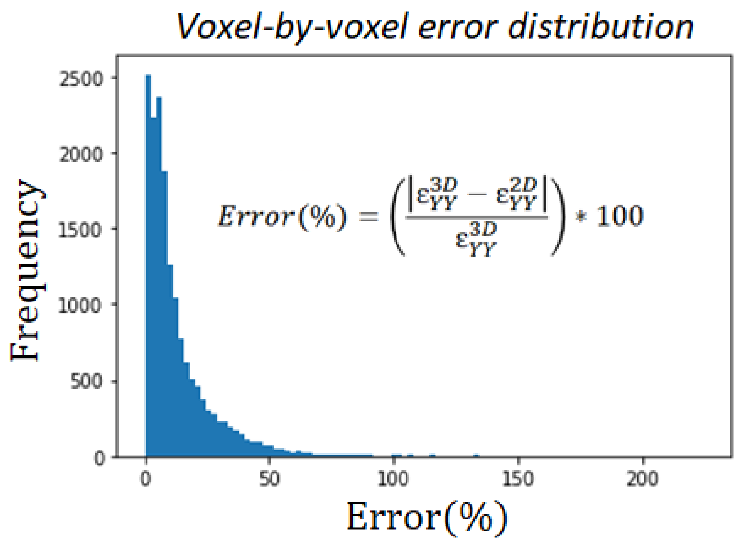

- Sub-surface microstructure influences strain accumulation on the free surface
- Hot spots identified from 2.5-dimensional (2.5D) simulations can be misleading
- Most of the voxels have errors within 10%
- However, significant errors (>50%) were observed in the strain map
- Influence of sub-surface microstructure and the errors associated with using 2.5D simulations needs to be kept in mind while comparing results with digital image correlation (DIC)
- This also underscores the importance of obtaining sub-surface microstructure

Validation of CPFE Simulations (AFRL AM 2020 Modeling Challenge)

Stress-strain curve

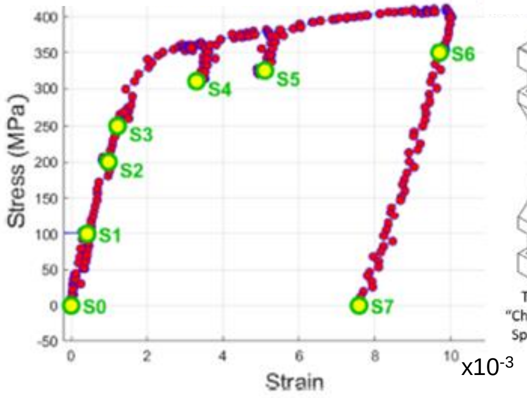

Tensile coupon

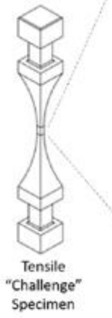

Serial-sectioned microstructure

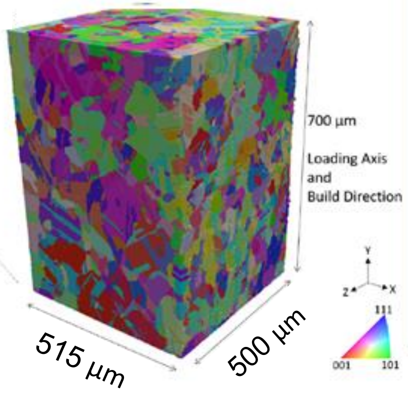

28 "challenge" grains

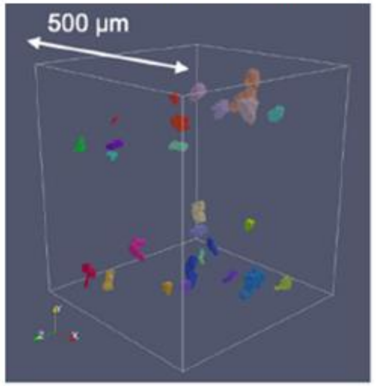

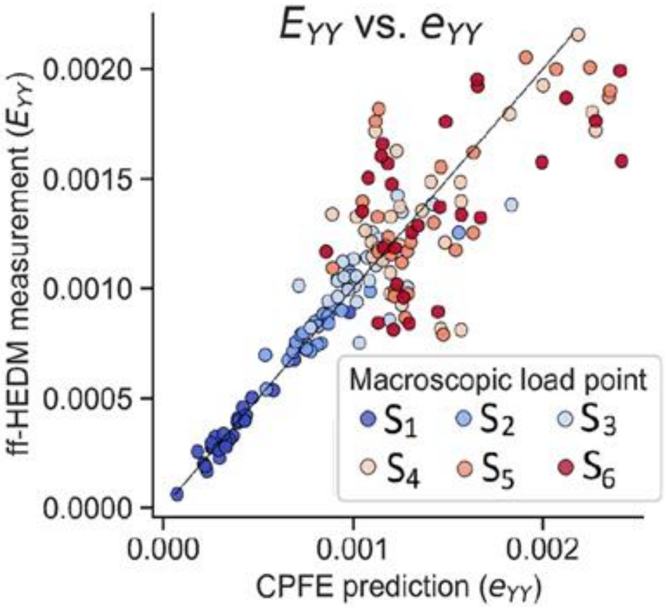

Challenge problem: Given the stress strain curve, serial-sectioned and reconstructed 3D microstructure, predict grain-average elastic strain tensor for 28 "challenge" grains at six different macroscopic load states, S1 through S6

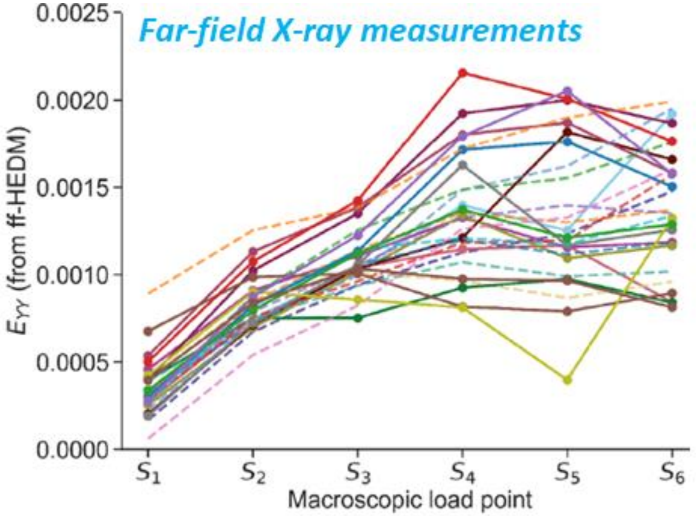

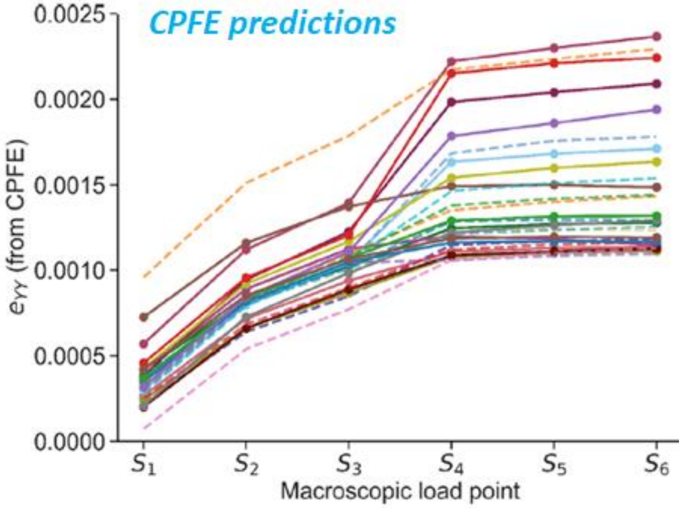

Validation of CPFE Simulations (NIST AM-Bench 2022 Challenge)

Challenge problem: Predict subcontinuum stress strain behavior, fracture location, and post failure width reduction of an as-built IN625 meso-scale specimen

AM-Bench challenge #:
CHAL-AMB2022-04-MeTT

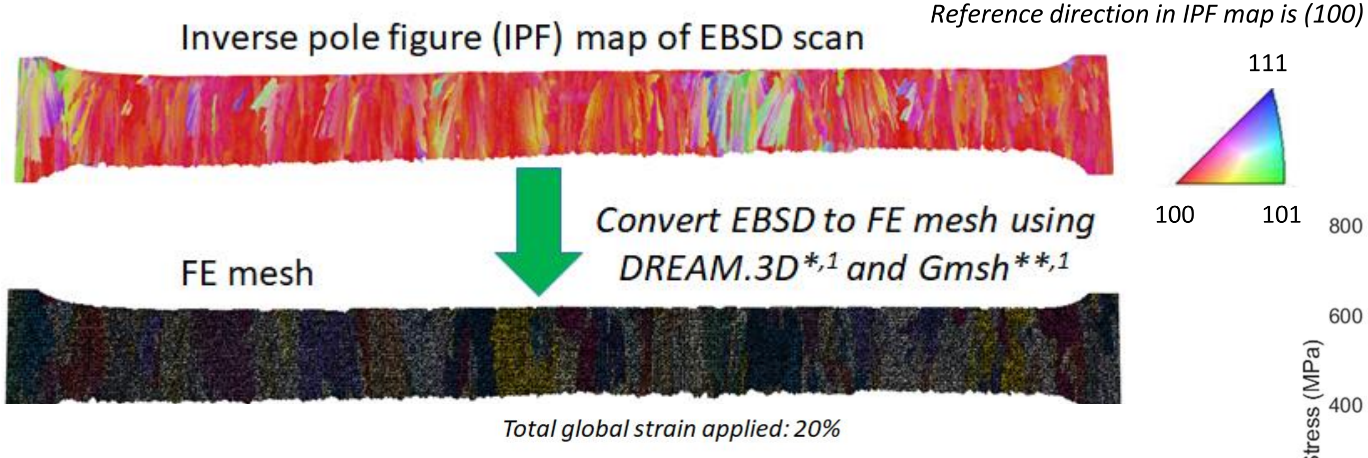

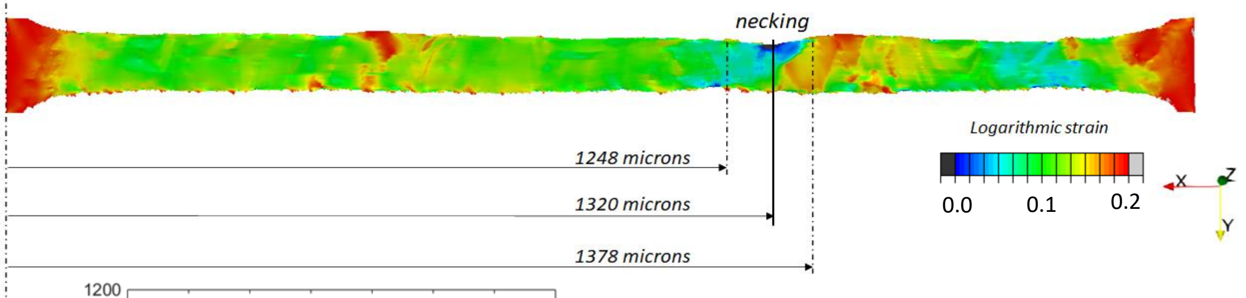

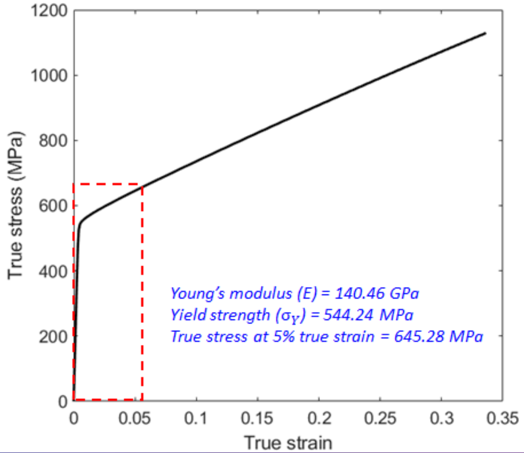

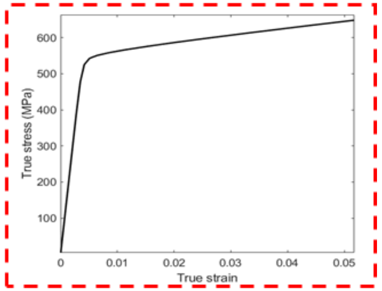

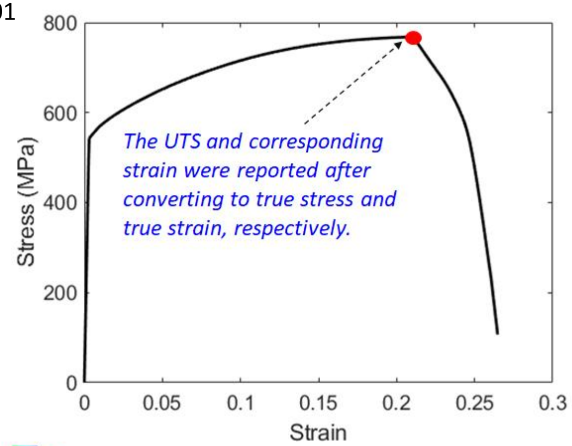

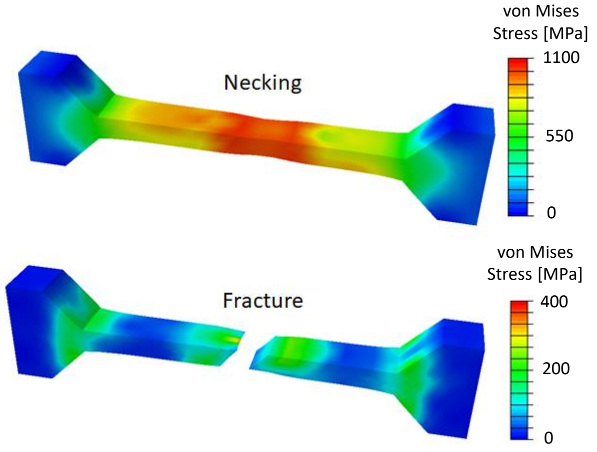

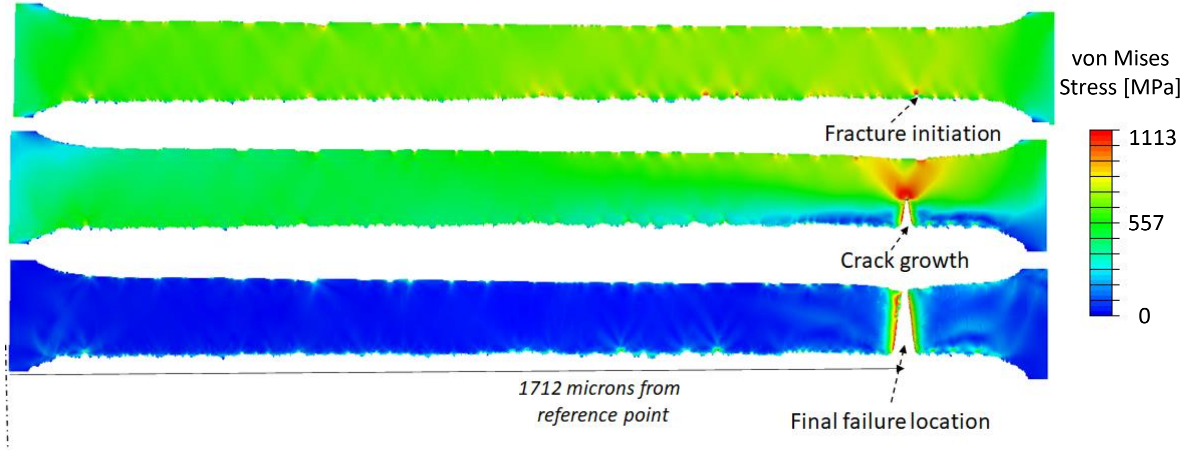

*http://dream3d.bluequartz.net
** https://gmsh.info

[1]This is not an endorsement by NASA

Validation of CPFE Simulations (NIST AM-Bench 2022 Challenge)

Challenge problem: Predict macroscale stress strain behavior of as-built Inconel-625 specimens extracted at various orientations to the build direction.

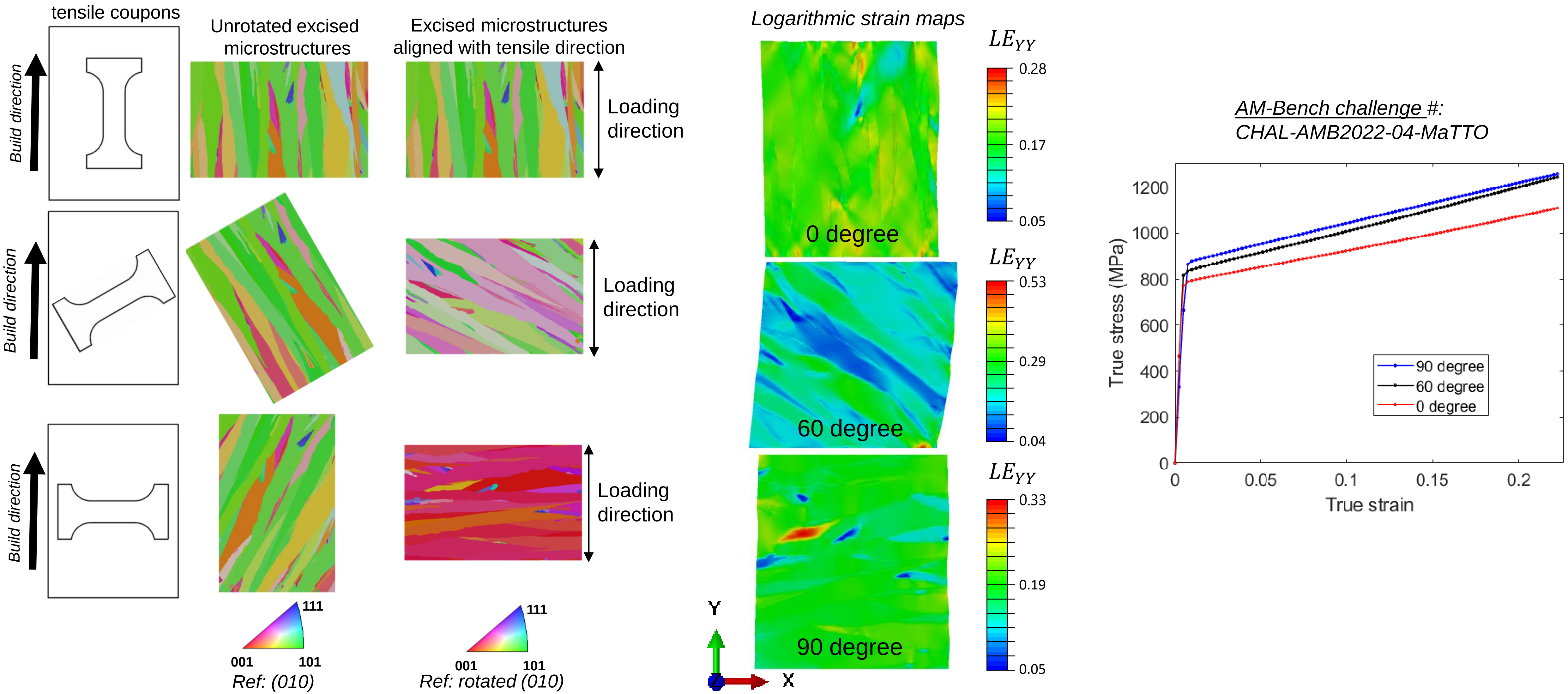

Acknowledgements

The work done was supported by the NASA Aeronautics Research Mission Directorate (ARMD) through the Transformational Tools and Technologies (T^3) project

Backup slides

Simulated 2-dimensional (2D) lack-of-fusion pores

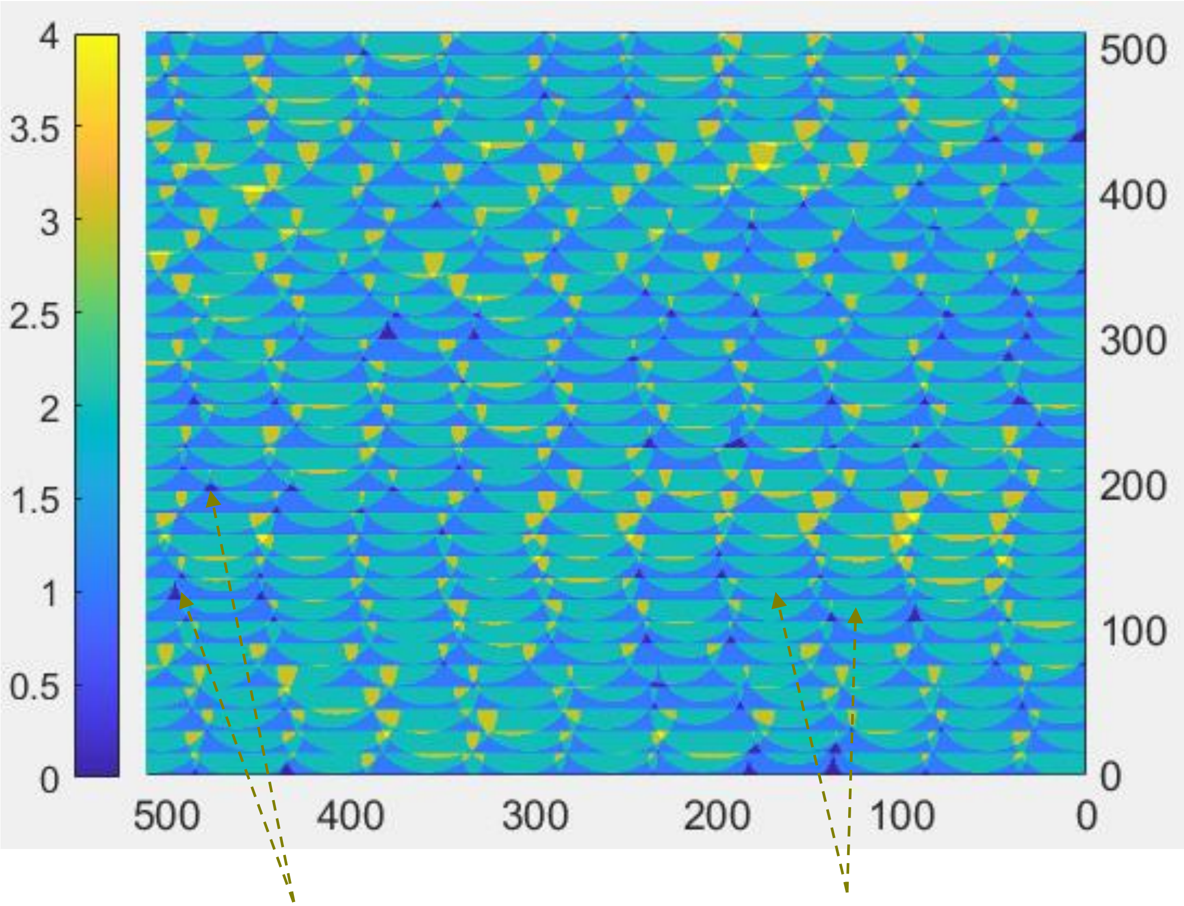

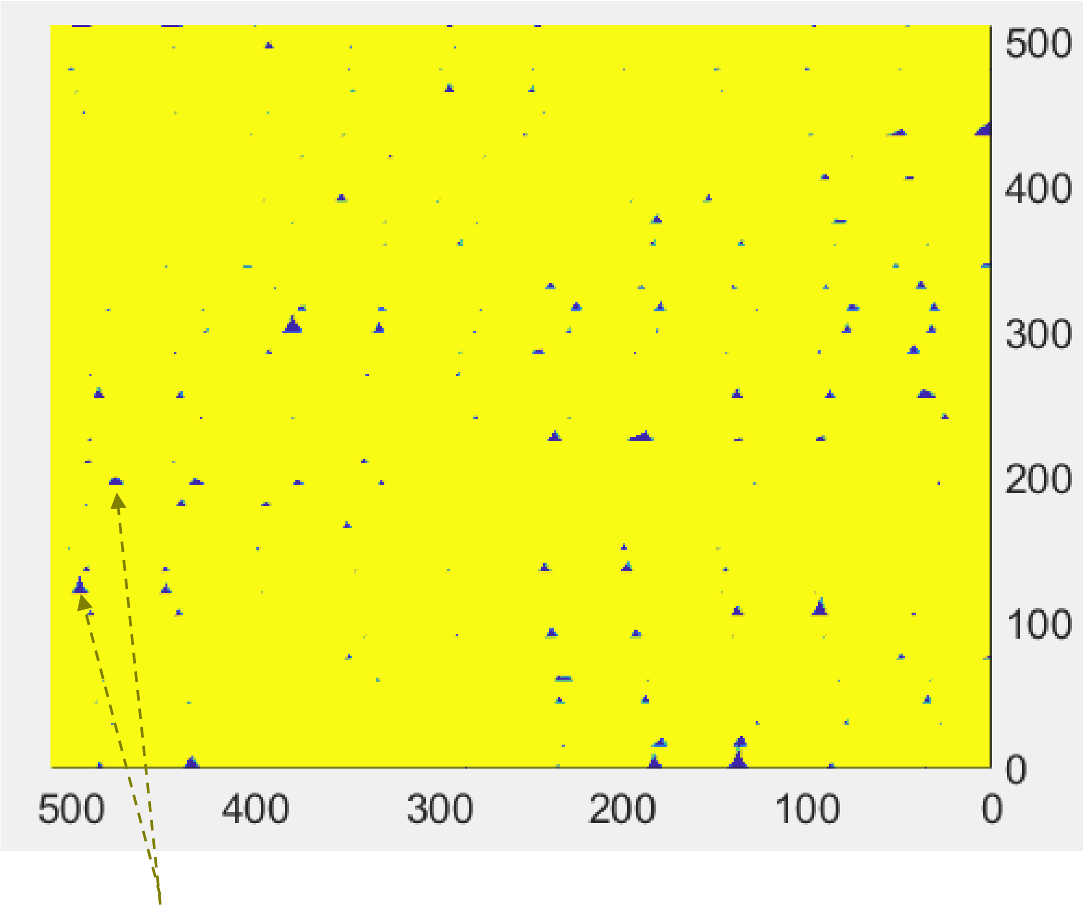

2D domain: 512x512 voxel^2
Resolution: 1 voxel = 2 microns

Influence of pore neighborhood

EBSD scan of additive Ti

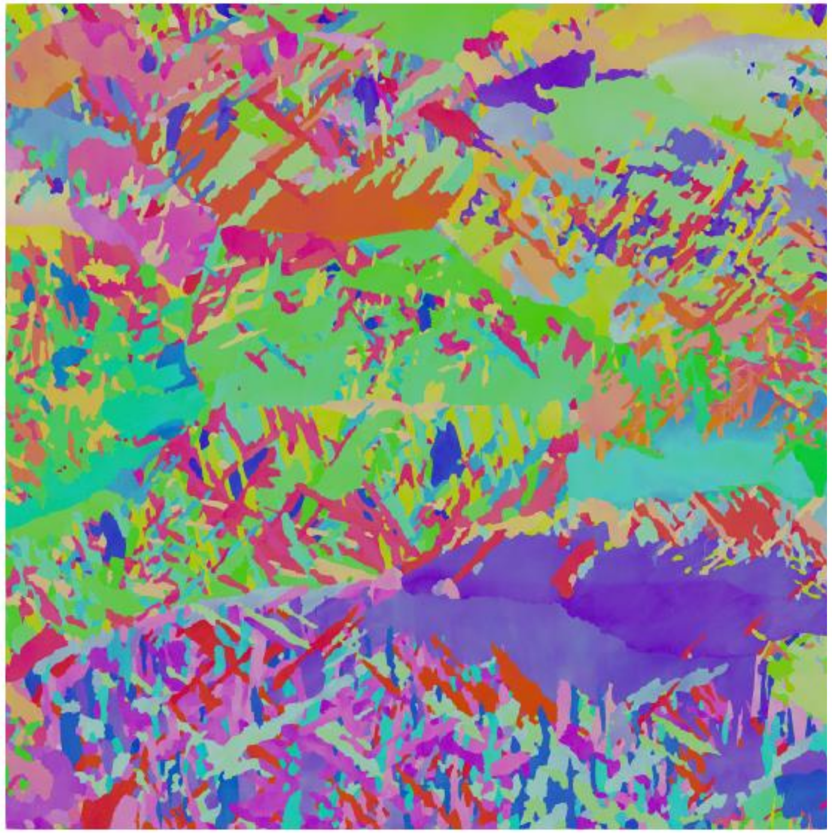

Courtesy: Wes Tayon

Microstructure only
(No defects)

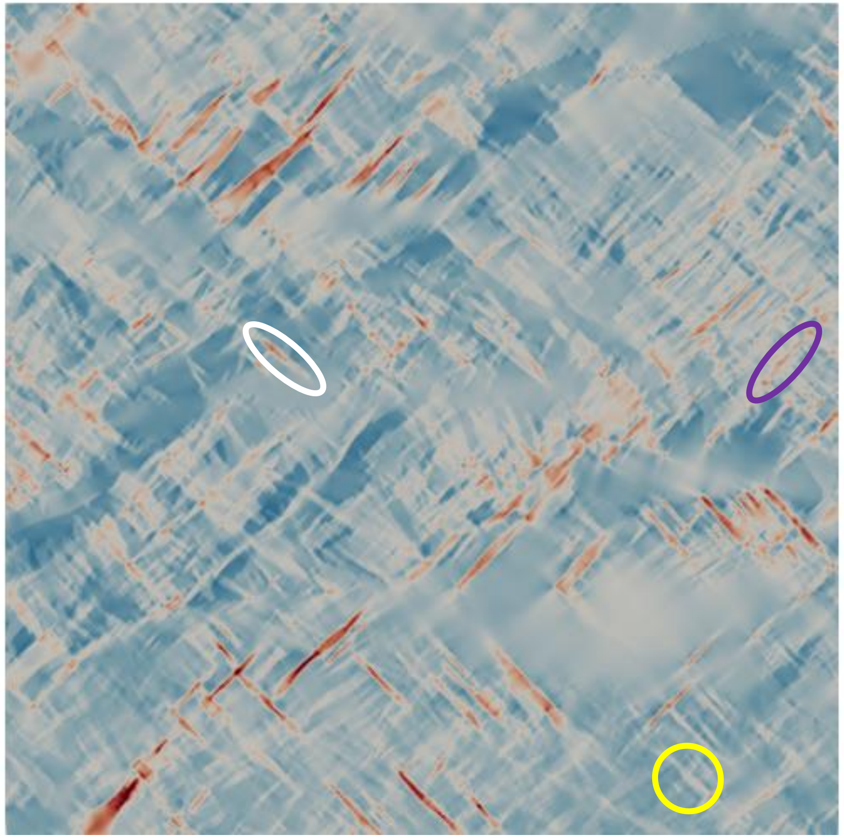

Microstructure + LoF pores

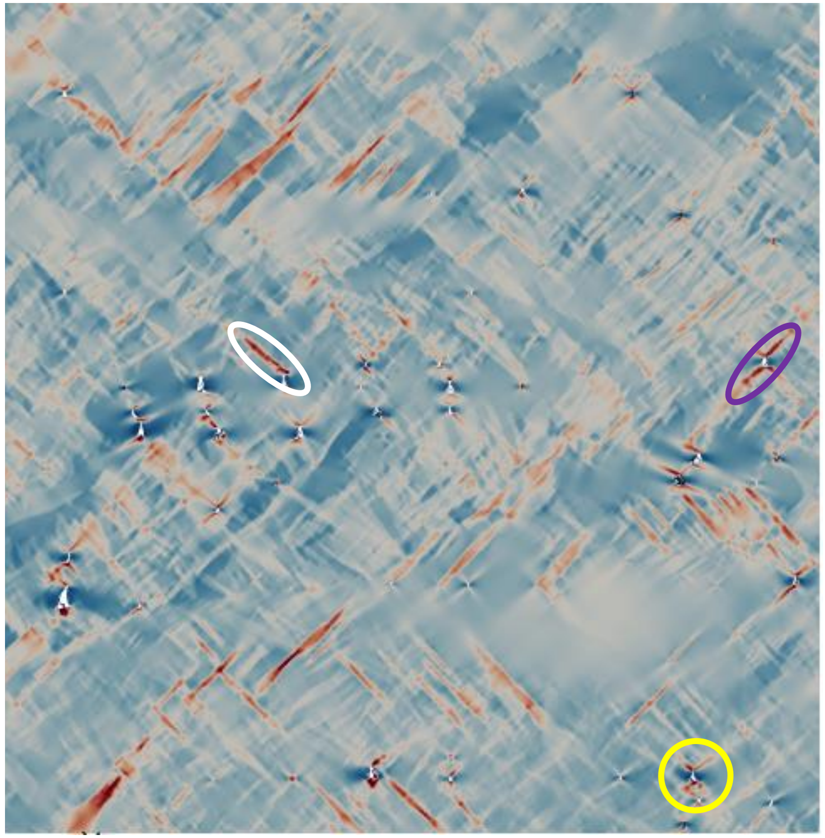

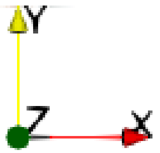

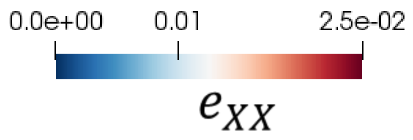

Loading direction: XX